

AFCRL-66-700

Antenna Laboratory Report No. 66-13

A NEAR-FIELD SOLUTION FOR AN INFINITE LINE  
SOURCE ABOVE A DIELECTRIC COATED CONDUCTING PLANE

by

G. F. Van Blaricum

R. Mittra

August 1966

Contract No. AF19(628)-3819

Project No. 5635

Task No. 563502

Technical Report No. 10

Prepared for

Air Force Cambridge Research Laboratories  
Office of Aerospace Research  
United States Air Force  
Bedford, Massachusetts 01730

Antenna Laboratory  
Department of Electrical Engineering  
University of Illinois  
Urbana, Illinois

DISTRIBUTION OF THIS DOCUMENT IS UNLIMITED

# ABSTRACT

The fields along a dielectric slab excited by a line source are found by considering the inversion integral of a Fourier transform directly rather than by resorting to the usual saddle point approximation techniques. The field at any point along the surface is expressed as a superposition of traveling waves plus a space-wave contribution, and conditions under which the field may be approximated by traveling wave components alone are discussed. Results of sample computations for both electric and magnetic current excitation are given.

## ACKNOWLEDGMENT

This work was supported in part by Air Force Cambridge Research Center under Contract AF19(628)-3819 and in part by the National Aeronautics and Space Administration under Grant NSG-395.

## TABLE OF CONTENTS

	Page
INTRODUCTION	1
DERIVATION OF THE FIELD SOLUTION	4
THE INVERSION INTEGRAL	10
BEHAVIOR OF THE INTEGRAND	16
COMPUTATIONS	22
RESULTS OF THE COMPUTATIONS	24
SUMMARY	34
BIBLIOGRAPHY	35

## LIST OF FIGURES

Figure		Page
1.	Grounded dielectric slab excited by a line source of current.	5
2.	Branch cuts and original path of integration.	11
3.	Deformed path of integration.	14
4(a).	Pole locations for $K = 2.5$ , $k_o = 3.0$ .	20
4(b).	Pole locations for $K = -0.5$ , $k_o = 3.0$ .	20
5(a).	Magnitude of vector potential, $k_o = 0.5$ .	25
5(b).	Magnitude of vector potential, $k_o = 1.0$ .	25
5(c).	Magnitude of vector potential, $k_o = 1.5$ .	26
5(d).	Magnitude of vector potential, $k_o = 2.0$ .	26
5(e).	Magnitude of vector potential, $k_o = 2.5$ .	27
5(f).	Magnitude of vector potential, $k_o = 3.0$ .	27
6(a).	Magnitude of vector potential, $k_o = 0.5$ .	28
6(b).	Magnitude of vector potential, $k_o = 1.0$ .	28
6(c).	Magnitude of vector potential, $k_o = 1.5$ .	29
6(d).	Magnitude of vector potential, $k_o = 2.0$ .	29
6(e).	Magnitude of vector potential, $k_o = 2.5$ .	30
6(f).	Magnitude of vector potential, $k_o = 3.0$ .	30
7(a).	Phase of vector potential for electric source, $k_o = 1.0$ .	31
7(b).	Phase of vector potential for magnetic source, $k_o = 3.0$ .	31
8(a).	Residue contribution and total field, $K = 2.5$ .	33
8(b).	Residue contribution and total field, $K = -0.5$ .	33

## INTRODUCTION

In many problems of electromagnetic theory, the solution may be obtained by transform techniques and it may be represented in terms of a contour integral, the so-called "inversion integral" of the transform, which is of the form

$$f(x,z) = \int_C g(x,\gamma) e^{-\gamma z} d\gamma$$

where  $x,z$  are the space variables,  $\gamma$  is the transform variable and  $C$  is the inversion contour. In some cases, the integral may be explicitly evaluated in terms of elementary functions, but frequently, only an approximate evaluation is possible. The most common approximation used involves an asymptotic evaluation of the far field. Since the asymptotic series involves inverse powers of  $r$ , the distance from the source, it is not very suitable for the calculation of near and intermediate range fields. This paper will present an approach for evaluating the fields at an arbitrary distance from the source along a surface wave structure.

The configuration is that of a grounded dielectric slab excited by a line source of magnetic or electric current. The standard analysis for such a problem, given in Collin<sup>2</sup> for the electric current source and later in this paper for the magnetic current source, reduces the solution for the fields to an inversion integral. The standard treatment of the integral is to carry out a change of variables and to approximate the far field by the saddle-point method of integration.

If only the radiation pattern is sought, it may be obtained immediately (for details, see Bates<sup>1</sup>) by evaluating the integrand at  $\gamma = j k \cos \theta$ , where  $\theta$  is the observation angle. However, it is frequently very useful to know the behavior of the fields at near and intermediate distances. For example, one can study coupling between two proximate antennas from knowledge of such fields. In particular, if the near-field behavior is describable as a superposition of traveling waves, the radiation pattern is easily obtained by the familiar Fourier transform relation, which is particularly simple in the case of exponentials. As an example, if the field behaves as  $\exp(-j\beta z)$ , where  $\beta = \beta_1 + j\beta_2$  is in general complex, then the radiation pattern is proportional to

$$|\beta - k \cos \theta|^{-1}$$

where  $k$  is the free-space propagation constant and  $\theta$  is the observation angle. Thus, the location and width of the maxima of the pattern are readily predictable from  $\beta_1$  and  $k$ .

Calculation of the near field in an analogous problem has been carried out previously by Norton<sup>4</sup> using the saddle-point method. Basically, the above approach was carried out with the addition of extra terms in the expansion of the integrand to make the approximation valid in the near field. The analytical results were shown to agree well with experimental data as near the source as one-half wavelength.

In this paper, the near field is determined by considering the inversion integral in a way which directly extracts the intermediate and far range

fields and simplifies computation of the near-field contribution. In addition, it obviates the necessity for the transformation of variables which is commonly introduced in the treatment of the integral (cf. Collin<sup>2</sup>). This method also expedites consideration of the field in terms of traveling wave components, and facilitates investigation of conditions under which the total field may be approximately given by the traveling wave components alone.



# DERIVATION OF THE FIELD SOLUTION

The geometry associated with the problem is shown in Figure 1. The dielectric slab has thickness  $t$  and dielectric constant  $K$ , and is infinite in extent in the  $y$  and  $z$  directions. At  $x = d$ , a unit current flows in the positive  $y$  direction.

The analysis presented here for a magnetic current source closely parallels that given in Collin<sup>2</sup> for an electric current. However, the problems are not duals.

From Maxwell's equations (assuming  $\exp(j\omega t)$  time variation)

$$\text{curl } \underline{E} = -j\omega\mu \underline{H} - \underline{K} \quad (1a)$$

$$\text{curl } \underline{H} = j\omega\epsilon \underline{E} \quad (1b)$$

we obtain the vector wave equation

$$\nabla^2 \underline{H} + k^2 \underline{H} = j\omega\epsilon \underline{K} \quad (2)$$

Because the magnetic current has only a  $y$  component, the vector electric potential also has only a  $y$  component.

$$\underline{E} = \text{curl } \underline{F} \quad (3a)$$

$$F_x = F_z = 0 \quad (3b)$$

If  $\psi(x,z) = \epsilon F_y$ , it follows that the only field components are given by:

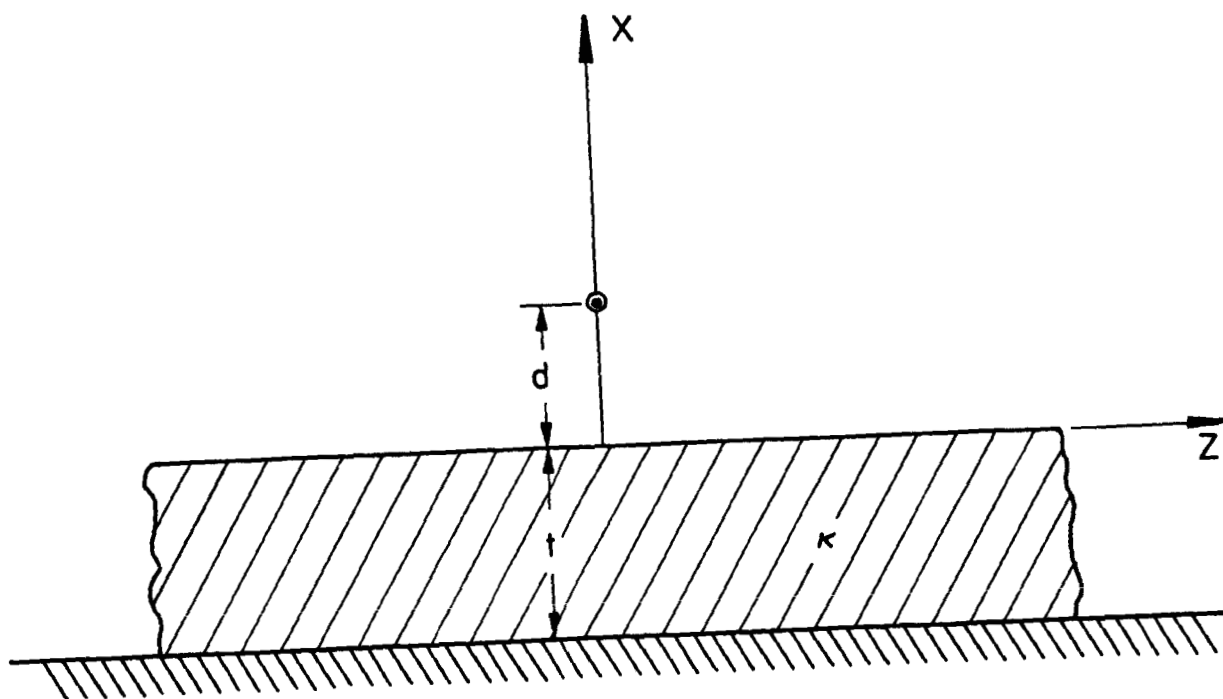


Figure 1. Grounded dielectric slab excited by a line source of current.

$$H_y = j \omega \psi \quad (4a)$$

$$E_z = \frac{1}{\epsilon} \frac{\partial \psi}{\partial x} \quad (4b)$$

$$E_x = - \frac{1}{\epsilon} \frac{\partial \psi}{\partial z} \quad (4c)$$

Assuming a source of unit strength, the function  $\psi$  must satisfy the differential equations

$$\nabla^2 \psi + k_o^2 \psi = \epsilon \delta(z) \delta(x - d) , \quad x > 0 \quad (5a)$$

$$\nabla^2 \psi + \kappa k_o^2 \psi = 0 , \quad -t < x < 0 \quad (5b)$$

Defining the bilateral Laplace transform

$$g(x, \gamma) = \int_{-\infty}^{\infty} \psi(x, z) e^{+\gamma z} dz \quad (6)$$

and transforming Equations (5a) and (5b) yields

$$\frac{d^2 g}{dx^2} + (\gamma^2 + k_o^2) g = \epsilon \delta(x - d) , \quad x > 0 \quad (7a)$$

$$\frac{d^2 g}{dx^2} + (\gamma^2 + \kappa k_o^2) g = 0 , \quad -t < x < 0 \quad (7b)$$

provided that the terms evaluated at  $\pm \infty$  in the integration by parts vanish. This corresponds to a slight loss in the medium, and implies that  $k_o$  must be complex instead of purely real.

If a solution for (7a) and (7b) is assumed to be of the form

$$g(x, \gamma) = C_1 \exp[jl(x - d)] \quad , \quad x \geq d \quad (8a)$$

$$= C_2 \exp[-jl(x - d)] \\ + C_3 \exp[jl(x + d)] \quad , \quad 0 \leq x \leq d \quad (8b)$$

$$= C_4 \sin(hx) + C_5 \cos(hx) \quad , \quad -t \leq x \leq 0 \quad (8c)$$

and the conditions

$$E_z = 0 \text{ at } x = -t \quad (9a)$$

$$E_z \text{ continuous at } x = 0 \quad (9b)$$

$$g \text{ continuous at } x = d \quad (9c)$$

$$\frac{dg}{dx} \text{ discontinuous by } \epsilon_0 \text{ at } x = d \quad (9d)$$

are satisfied, the solution is

$$g(x, \gamma) = \frac{j\epsilon_0}{2l} \left\{ 1 + R_1 \exp(2jld) \right\} \exp[jl(x - d)] \quad , \quad x \geq d \quad (10a)$$

$$= \frac{j\epsilon_0}{2l} \left\{ \exp[-jl(x - d)] + R_1 \exp[jl(x + d)] \right\} \quad , \quad 0 \leq x \leq d \quad (10b)$$

$$= \frac{j\epsilon_0 [-\sin(hx) + \cot(ht)\cos(hx)] \exp(jld)}{\left[ \frac{jh}{K} - l \cot(ht) \right]} \quad , \quad -t \leq x \leq d \quad (10c)$$

where

$$h^2 = \gamma^2 + \kappa k_o^2$$

$$\ell^2 = \gamma^2 + k_o^2$$

$$R_1 = \frac{j\ell - \frac{h}{\kappa} \tan(ht)}{j\ell + \frac{h}{\kappa} \tan(ht)}$$

For  $x \geq 0$ ,  $g$  may be written in the more compact form

$$g(x, \gamma) = -\frac{j\epsilon_o}{2\ell} [\exp(j\ell|x-d|) + R_1 \exp(j\ell|x+d|)] \quad (11)$$

Inverting the transform yields the expression

$$\psi(x, z) = \frac{-\epsilon_o}{4\pi} \int_C [\exp(j\ell|x-d|) + R_1 \exp(j\ell|x+d|)] \frac{\exp(-\gamma z)}{\ell} d\gamma \quad (12)$$

for an appropriate contour  $C$ . In addition, particular care must be exercised in selecting the proper branch of the square-root function to insure satisfaction of the radiation condition. That branch of the square-root function must be chosen which yields a positive imaginary part for  $\ell = (\gamma^2 + k_o^2)^{\frac{1}{2}}$ . Henceforth, that branch will be referred to as the proper branch, and the one yielding a negative imaginary part will be called the improper branch.

Analysis in Collin<sup>2</sup> for the case of a line source of electric current yields

$$\phi(x, z) = \frac{\mu_o}{4\pi} \int_C [\exp(j\ell|x-d|) + R \exp(j\ell|x+d|)] \frac{\exp(-\gamma z)}{\ell} d\gamma \quad (13)$$

where  $\phi(x, z) = y$  component of the magnetic potential,

$$R = \frac{h \cot(ht) + j\ell}{-h \cot(ht) + j\ell}$$

and the proper branch of the square-root function is chosen.

For the special case  $x = 0$ , Equations (12) and (13) simplify to

$$\psi(0, z) = \frac{-\epsilon_0}{4\pi} \int_C \frac{2j \exp(j\ell d - \gamma z)}{j\ell + \frac{h}{k} \tan(ht)} d\gamma \quad (14)$$

$$\phi(0, z) = \frac{\mu_0}{4\pi} \int_C \frac{2j \exp(j\ell d - \gamma z)}{j\ell - h \cot(ht)} d\gamma \quad (15)$$

## THE INVERSION INTEGRAL

Formally, the inversion contour  $C$  must lie in a strip where the integrand is holomorphic, and  $C$  must not cross a branch cut. In general, the integrands have poles at  $\gamma = \pm j k_0$ , so that if  $k_0$  is slightly complex, the imaginary axis of the  $\gamma$ -plane is a suitable contour. This complex value of  $k_0$  also satisfies the condition mentioned in the preceding section requiring that certain terms vanish in the transformation of the differential equation. (In the discussion from this point on, however,  $k_0$  will be treated as if it were purely real. Statements about poles on the imaginary axis and about deformations of the contour  $C$  to include or exclude poles on the axis correspond in actuality to limiting cases as the loss in the medium is made vanishingly small. In all cases, slight loss is needed to maintain rigor, but it adds an unnecessary complication to most of the discussion.)

The branch points at  $\pm j k_0$  must be connected by a branch cut separating the proper from the improper branch of the square-root function. Because the contour  $C$  may not cross a branch cut, the branch points must be connected by a cut which passes through the point at infinity. Collin<sup>2</sup> discusses the possibility of choosing various branch cuts, finally selecting the locus of points satisfying  $\text{Im}(\gamma^2 + k_0^2)^{\frac{1}{2}} = 0$ , which for the lossy medium is hyperbolic. As the loss is made very small, the branch cut approaches that shown in Figure 2. Crossing the branch cut corresponds to switching from the proper to the improper branch of the square root, so that the  $\gamma$ -plane may be regarded as a Riemann surface of two sheets, the top sheet corresponding to the proper branch of the square root and the bottom sheet to the improper branch. The contour  $C$  lies entirely in the top sheet.

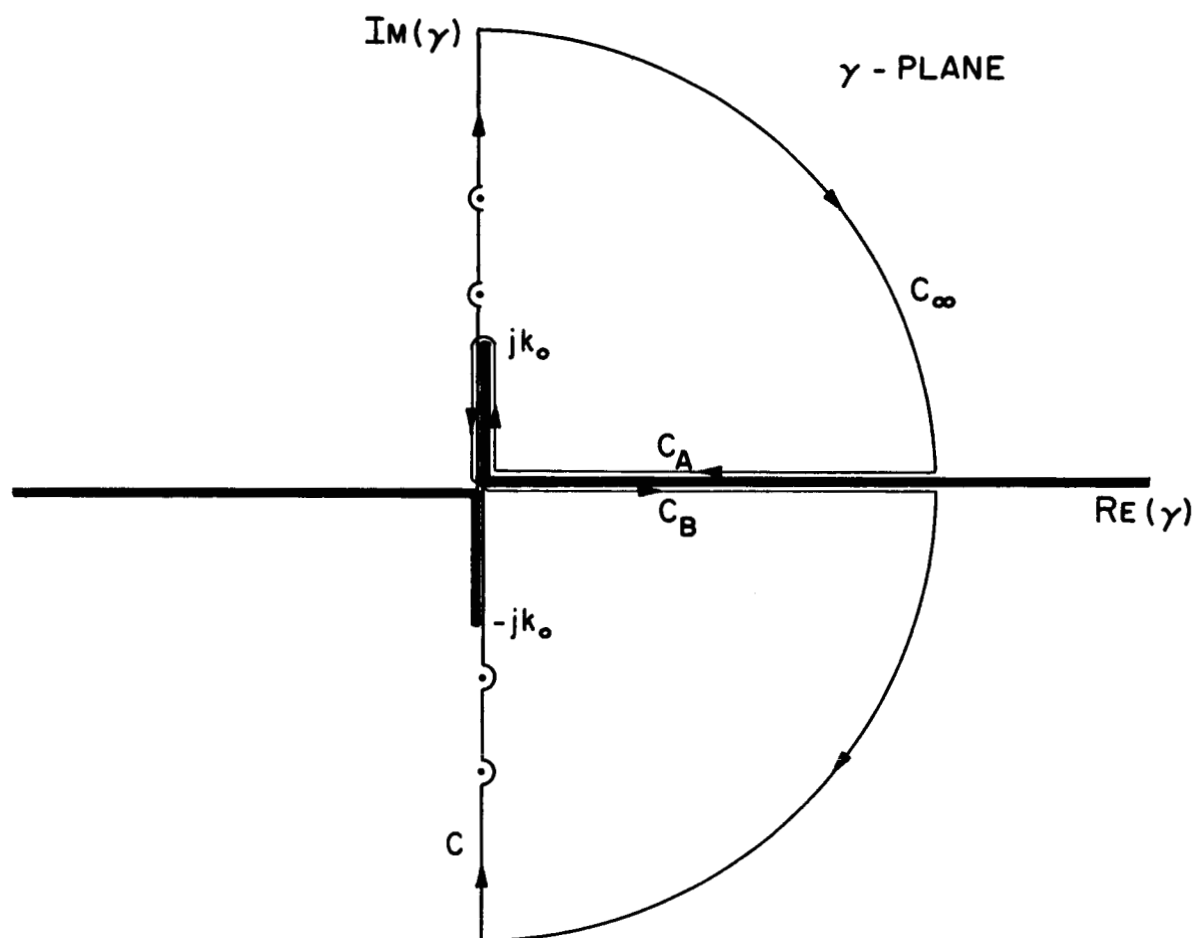


Figure 2. Branch cuts and original path of integration.



In order to evaluate the integral along the path C, the contour is closed in the right half-plane (for  $z > 0$ ) as in Figure 2. By the Cauchy integral formula,<sup>3</sup>

$$\int_C = - \int_{C_\infty} - \int_{C_A} - \int_{C_B} - 2\pi j \sum \text{residues} \quad (16)$$

For  $x = 0$ , the integral along  $C_\infty$  vanishes for all  $z > 0$ . Now the original integral is equal to the branch cut integral, which represents the space wave with a continuous eigenvalue spectrum, plus the residues at the enclosed poles, which represent traveling waves on the surface with a discrete eigenvalue spectrum.

The usual procedure at this point is to execute a change of variables, letting,

$$\gamma = j k_0 \sin \xi \quad (17)$$

where

$$\xi = \eta + j \zeta \quad (18)$$

Then in the  $\xi$ -plane, a stationary point (which must be a saddle point because holomorphic functions do not possess maxima and minima<sup>3</sup>) is found, and the transformed path of integration C is deformed in the  $\xi$ -plane to pass through the saddle point on the steepest-descent path. The integrand is then expanded in a Taylor series about the saddle point, and the integral

along the contour is evaluated in some manner. In addition, the residue contributions of the poles of the integrand crossed in deforming the contour of integration are added to the result.

In Norton's<sup>4</sup> treatment of the near field in a similar structure, he noted that in addition to the residues, the poles lying near the saddle point and steepest-descent path, even though they may not be enclosed by the contour, do in fact contribute to the field by influencing the behavior of the integrand along the path of integration. By accounting for these in a Laurent series about the pole location, he was able to determine the field as near as one-half wavelength to the source.

However, the evaluation of the inversion integral may be considered entirely in the  $\gamma$ -plane. The branch cut integrals along  $C_A$  and  $C_B$  are deformed into integrals along  $C_{A'}$  and  $C_{B'}$  as shown in Figure 3. Along these segments, the integrand decays exponentially. In deforming the contour into that shown in Figure 3, the contour crosses the branch cut into the bottom sheet of the Riemann surface, so that residues at poles in the strip,  $0 \leq \text{Im}(\gamma) \leq k_0$ ,  $0 \leq \text{Re}(\gamma)$ , of the bottom sheet must be considered. Now,

$$\begin{aligned}
 \int_C &= - \int_{C_\infty} - \int_{C_{A'}} - \int_{C_{B'}} \\
 &\quad - 2\pi j \sum \quad (\text{residues enclosed on top sheet}) \\
 &\quad - 2\pi j \sum \quad (\text{residues enclosed on bottom sheet})
 \end{aligned}
 \tag{19}$$

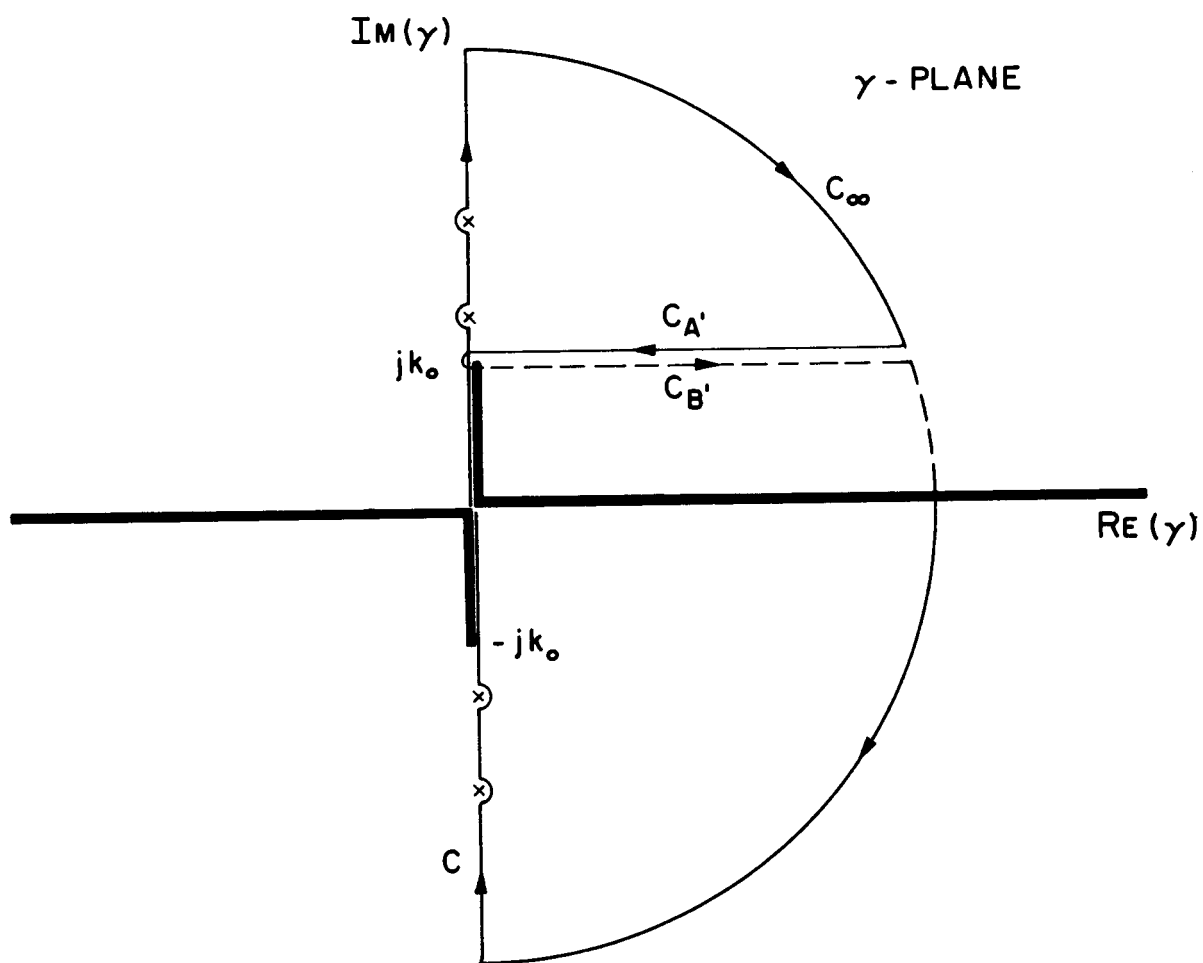


Figure 3. Deformed path of integration.

Staying in the  $\gamma$ -plane to perform the integration has certain advantages over integrating in the transformed  $\xi$ -plane. First, the path is a straight line, which is convenient for numerical evaluation of the integrals. (It may be interesting to note that this path of integration is very close to the steepest-descent path for all distances along the surface except in the neighborhood of  $z = 0$ .) Secondly, it is quite easy to define the region in which to search for poles crossed in deforming the contour, since it is a semi-infinite strip in the bottom sheet of the Riemann surface. Also, determining at what point to neglect poles in the strip is simplified, as will be shown in the discussion of the behavior of the integrand in the next sections.

## BEHAVIOR OF THE INTEGRAND

The poles of the integrands in (14) and (15) are the zeros of

$$j(\gamma^2 + k_o^2)^{\frac{1}{2}} + \frac{1}{K} (\gamma^2 + K k_o^2)^{\frac{1}{2}} \tan[(\gamma^2 + K k_o^2)^{\frac{1}{2}} t] \quad (20a)$$

and

$$j(\gamma^2 + k_o^2)^{\frac{1}{2}} - (\gamma^2 + K k_o^2)^{\frac{1}{2}} \cot[(\gamma^2 + K k_o^2)^{\frac{1}{2}} t] \quad (20b)$$

for magnetic current and electric current, respectively. Since the contour of integration has been deformed to enclose a strip of the bottom sheet of the Riemann surface, roots corresponding to both branches of the square-root function must be found.

On the top sheet, letting  $y^2 = (K - 1) k_o^2 t^2 - h^2 t^2$ , roots of (20a) and (20b) are simultaneous solutions of

$$\begin{cases} \left(\frac{ht}{K}\right) \tan(ht) = y \\ (ht)^2 + y^2 = (K - 1) k_o^2 t^2 = r^2 \end{cases} \quad (21a)$$

and

$$\begin{cases} (ht) \cot(ht) = -y \\ (ht)^2 + y^2 = (K - 1) k_o^2 t^2 = r^2 \end{cases} \quad (21b)$$

respectively.

Plotting graphs of these equations in  $(ht)$  and  $y$ , and solving for  $\gamma$ , shows that:

1. No solutions of this type occur for  $K < 1$ , because the radius  $r$  must be real.
2. For electric excitation, no solutions occur for  $(K - 1)^{\frac{1}{2}} k_0 t < 1$  because the circles do not intersect the curve  $(ht) \cot (ht)$  unless the radii are at least unity.
3. Values of  $\gamma$  which are solutions are purely imaginary, and solutions occur in conjugate pairs.
4. For each value of  $K$  and  $k_0$ , there are only finitely many simultaneous solutions of the pairs of equations.

Calculating the residues at the poles corresponding to these purely imaginary values of  $\gamma$  yields a factor proportional to  $\exp(-\gamma z)$ . If  $\gamma = \pm j\beta$ , the  $+$  sign corresponds to a wave propagating in the  $+z$  direction without attenuation but evanescent in the  $+x$  direction, i.e., a surface wave. In order to exclude the waves propagating in the  $-z$  direction, the contour of integration  $C$  along the imaginary axis must be deformed slightly to include the poles on the positive imaginary axis and to exclude those on the negative imaginary axis.

For the slab with  $K = -0.5$ , excited by a magnetic current, there exist in the top sheet a set of poles which have positive real parts and negative imaginary parts, corresponding to waves decaying in the  $+z$  direction, but with a phase variation in the opposite sense. (To see the influence of such poles in the field solution, see Figure 7(b) for  $K = -0.5$ .) There are

infinitely many of these "backward wave" poles, and asymptotically, their separation is  $\pi/t$ . Because the residues are proportional to  $\exp(-\gamma z)$ , though, for non-zero values of  $z$ , only the contributions of the first few with smallest real parts are significant.

On the bottom sheet, there exist an infinite number of complex roots of (20a) and (20b). However, only those within the strip  $0 \leq \text{Im}(\gamma) \leq k_0$ ,  $0 \leq \text{Re}(\gamma)$  are enclosed by the contour of integration. If there are infinitely many of these poles within the strip, the distance between adjacent poles is given by  $\pi/t$ . As before, the residues vary as  $\exp(-\gamma z)$ , so that only the first few need be considered. These poles are commonly called leaky wave\* poles.

These leaky wave poles appear to contribute terms to the field expansion which, although properly behaved in  $z$ , appear to grow without bound in  $x$ . However, it must be recalled that the leaky wave residues plus the integrals along  $C_A$  and  $C_B$  represent the original branch cut integral, and constitute the space wave. Leaky waves permit partial expansion of the fields in terms of the traveling wave behavior convenient for investigation. Even though one cannot continue to use the leaky wave representation for arbitrary distances from the source at arbitrary observation angles, this representation is certainly valid along the surface. From knowledge of the fields along the surface, one can then use Huygen's principle<sup>6</sup> to evaluate the far fields at arbitrary observation angles.

---

\* Tamir, T. and Oliner, A. A., "Guided Complex Waves, Part I," Proc. IEE (London), 110, No. 2, 1963, pp. 310-324.

Leaky wave poles near the path  $C_B$ , can also contribute to the field expansion by influencing the behavior of the integrand. Additional complex poles on the bottom sheet which are not within the strip may also influence the behavior of the integrand, so that if it is desired to express the fields only in terms of traveling waves and to neglect the radiated field, careful investigation of additional complex poles in the bottom sheet helps in determining conditions under which the integral may be neglected.

It has been shown by Bates<sup>1</sup> that for slabs with dielectric constant greater than unity, all complex roots must lie on the bottom sheet of the Riemann surface. It is suspected that the same result holds for all non-negative values of  $K$ , and numerical calculations for several cases with  $K = 0.5$  tend to confirm this. However, for  $K = -0.5$ , backward wave poles occurred in the top sheet, so that the result is not true in general. Backward wave modes were not excited, though, by the electric current in the cases considered.

In Figures 4(a) and 4(b), locations of the surface wave, leaky wave and backward wave poles are shown for two sets of parameters. Table 1 summarizes the types of poles found for several cases of both electric and magnetic excitation.



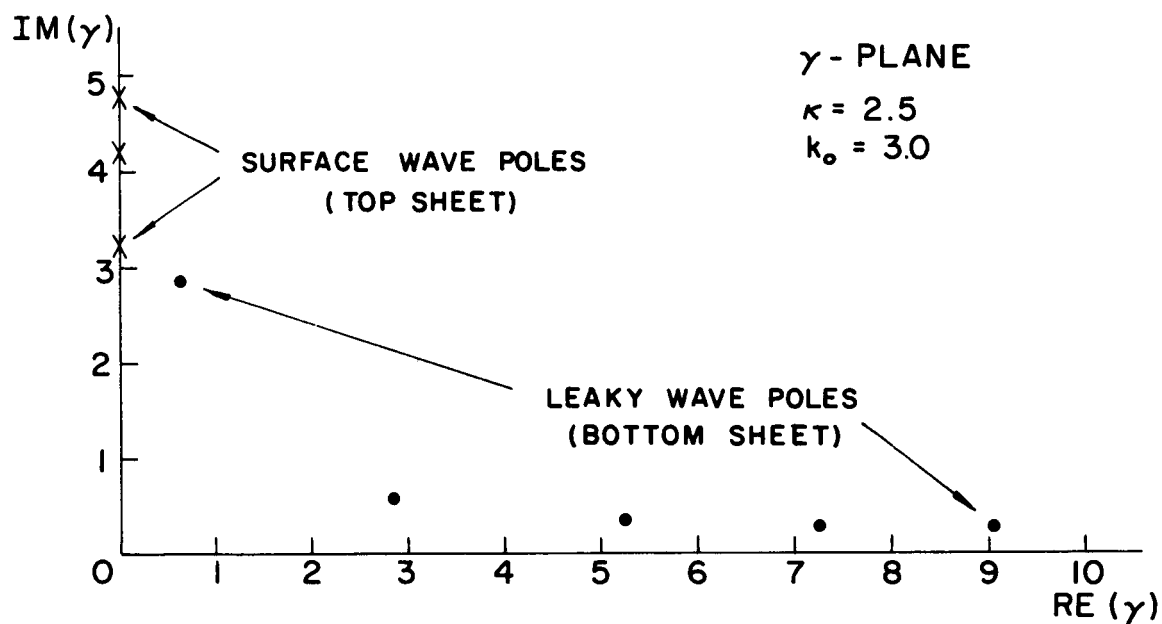


Figure 4(a). Pole locations for  $\kappa = 2.5$ ,  $k_0 = 3.0$ .

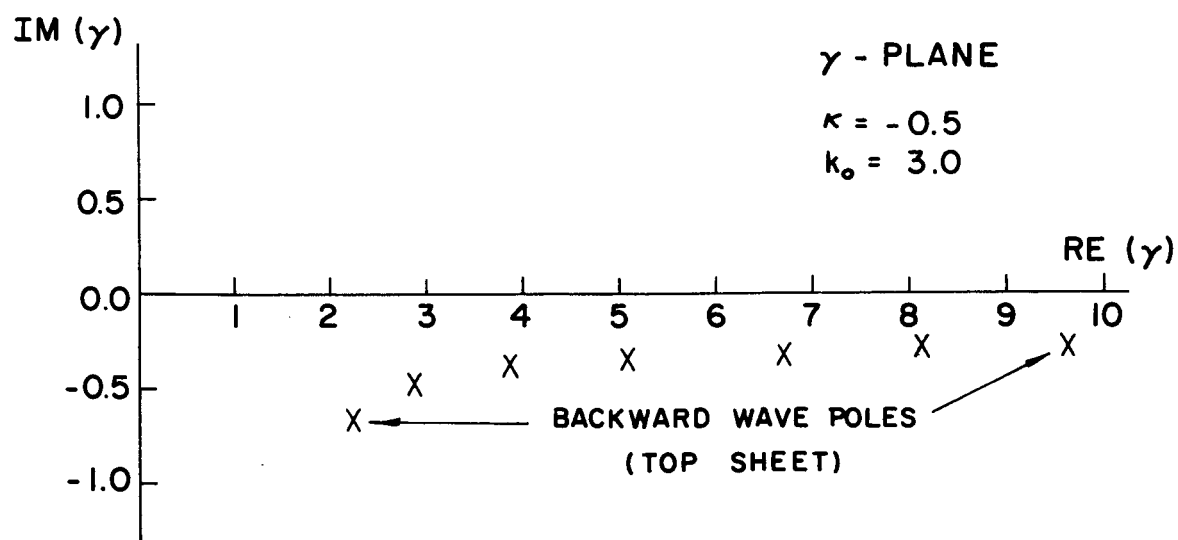


Figure 4(b). Pole locations for  $\kappa = -0.5$ ,  $k_0 = 3.0$ .

TABLE 1

## TYPES OF POLES FOR VARIOUS PARAMETERS AND EXCITATIONS

Excitation	$K$	$k_0$	Surface Waves	Leaky Waves	Backward Waves
Electric	2.5	0.5	No	No	No
Electric	2.5	1.5	Yes	Yes	No
Electric	2.5	2.5	Yes	Yes	No
Electric	0.5	1.5	No	No	No
Electric	0.5	1.5	No	Yes	No
Electric	0.5	2.5	No	Yes	No
Electric	-0.5	0.5	No	No	No
Electric	-0.5	1.5	No	Yes	No
Electric	-0.5	2.5	No	Yes	No
Magnetic	2.5	0.5	Yes	Yes	No
Magnetic	2.5	1.5	Yes	Yes	No
Magnetic	2.5	2.5	Yes	Yes	No
Magnetic	0.5	0.5	No	Yes	No
Magnetic	0.5	1.5	No	Yes	No
Magnetic	0.5	2.5	No	Yes	No
Magnetic	-0.5	0.5	No	No	Yes
Magnetic	-0.5	1.5	No	No	Yes
Magnetic	-0.5	2.5	No	No	Yes

## COMPUTATIONS

The computation of  $\psi$  and  $\phi$  for magnetic and electric excitation, respectively, was divided into two main parts--location of poles of the integrand and calculation of residues at these poles, and computation of the integrals on  $C_{A^*}$  and  $C_{B^*}$ .

In order to find the poles of the integrands, i.e., zeros of (20a) and (20b), it was found necessary to make very close estimates of the actual locations. To secure these estimates, values of Equations (20a) and (20b) were calculated at points of a fine grid in the regions where roots were being sought. The signs of the real and imaginary parts were studied to determine points at which both parts changed sign simultaneously. Once estimates of the zero locations were found, these estimates were used in the Newton-Raphson method,<sup>5</sup> modified for complex arithmetic, to find the values to greater precision. To obtain the locations of surface wave poles, graphical solutions of (21a) and (21b) provided good estimates, and the Newton-Raphson method was again used to provide more precise values. For leaky wave and backward wave poles, it was observed that the residues decayed exponentially, so that for a fixed lower bound on  $z$ , an upper bound on the real part of  $\gamma$  could be easily determined such that residues at poles with greater real parts would be negligibly small. Thus, in each instance, the regions in which poles were sought were rectangular regions of the  $\gamma$ -plane.

Calculation of the integrals along  $C_{A^*}$  and  $C_{B^*}$  was done using a

modification of RIEMAN,\* a FORTRAN II subroutine for numerical integration. Provided with a given error bound, RIEMAN divides the interval of integration into subdivisions of proper size to assure an answer within the given error limit.

Along  $C_A$  and  $C_B$ , the integrand decays at least as rapidly as  $\exp(-\alpha z)$ , where  $\gamma = \alpha + j k_0$  on  $C_A$  and  $C_B$ . If the infinite path of integration is replaced by the finite segment from  $0 + j k_0$  to  $\alpha_1 + j k_0$ , where  $\alpha_1$  is chosen so that, say,  $\alpha_1 z > 10$ , the error introduced is quite small. The integrals were approximated by integrals along such finite segments. Several cases were checked by extending the length of the interval of integration by at least fifty per cent; no significant difference in the values obtained was noted.

All computations were made on the IBM 7094 computer of the University of Illinois Department of Computer Science. All programming was done in FASTRAN, a fast-compiling version of FORTRAN II.

---

\* Russell, David L., "AND 107 Numerical Integration Using Midpoint Procedure with Preferential Interval Placement," Argonne National Laboratory, Applied Mathematics Division, August 1960.

## RESULTS OF THE COMPUTATIONS

Results of computations for the various choices of wave number and dielectric constant, for both magnetic and electric excitation, are shown in Figures 5(a) - 5(f), 6(a) - 6(f) and 7(a) - 7(b). In every case, the parameters  $t$ , the thickness of the slab, and  $d$ , the height of the source above the slab, were fixed ( $t = 2$ ,  $d = 0.1$ ). The quantities plotted in Figures 5 and 6 are the magnitudes of the  $y$  component of the vector potential. The phases of selected cases are given in Figures 7(a) and 7(b).

As would be intuitively expected, the field grows quite large as  $z$  becomes small. These results agree well in their general behavior with those obtained by Norton<sup>4</sup> both analytically and experimentally in an analogous problem. For the cases in which no poles of the integrand were found, it was possible to directly compute the inversion integral along  $C$  for  $z = 0$ ,  $0.1$  and  $0.25$ . The values so obtained agree extremely well with the extrapolation of the respective curves to zero. For other cases, however, direct computation of the inversion integral for  $z = 0$  yielded values much smaller than would otherwise have been expected. It is uncertain in these cases whether the apparent inconsistencies arise from errors in the computation of the inversion integral introduced by poles on the path of integration (which are avoided by slightly deforming the path) or whether the fields in fact peak for some very small value of  $z$  and decrease as  $z$  approaches zero. In one of the cases measured by Norton,<sup>4</sup> such behavior is in fact evidenced, as the field peaked and then decreased sharply for smaller values of  $z$ . The behavior evinced in Figure 6(e)

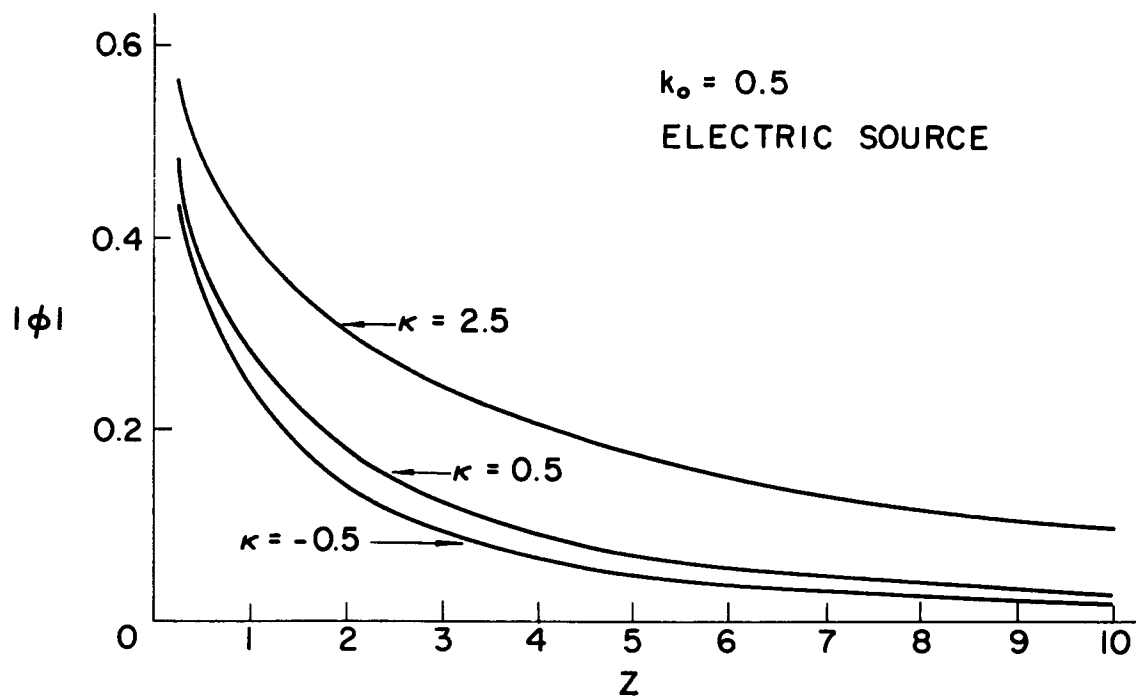


Figure 5(a). Magnitude of vector potential,  $k_0 = 0.5$ .

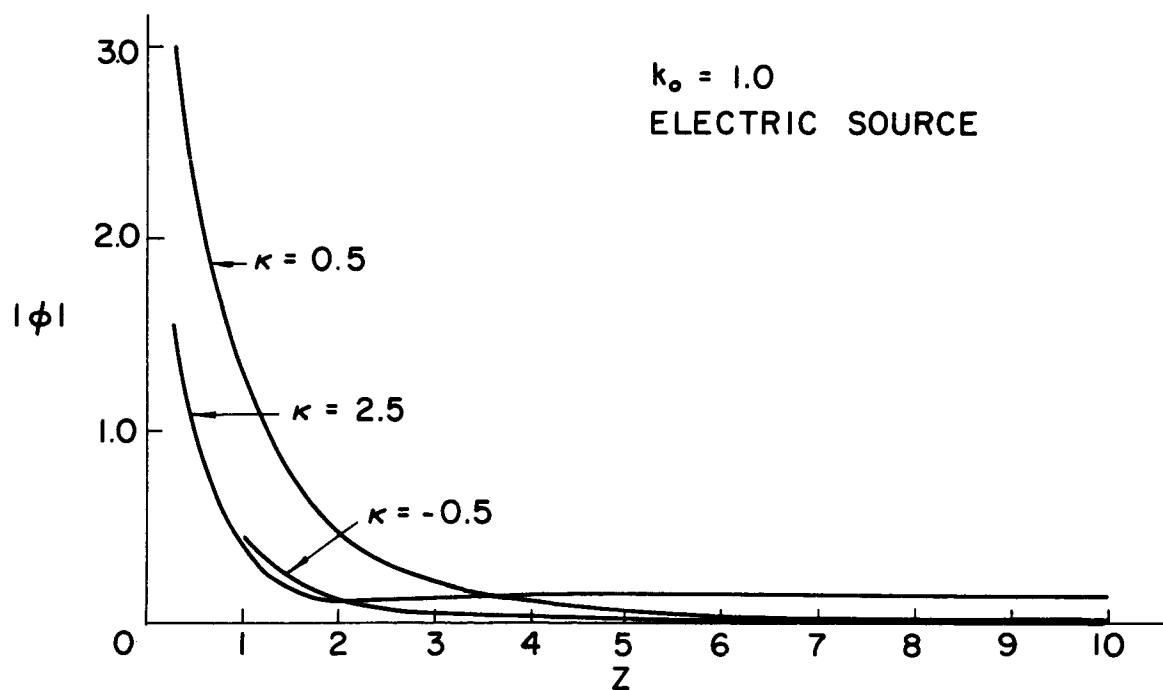


Figure 5(b). Magnitude of vector potential,  $k_0 = 1.0$ .

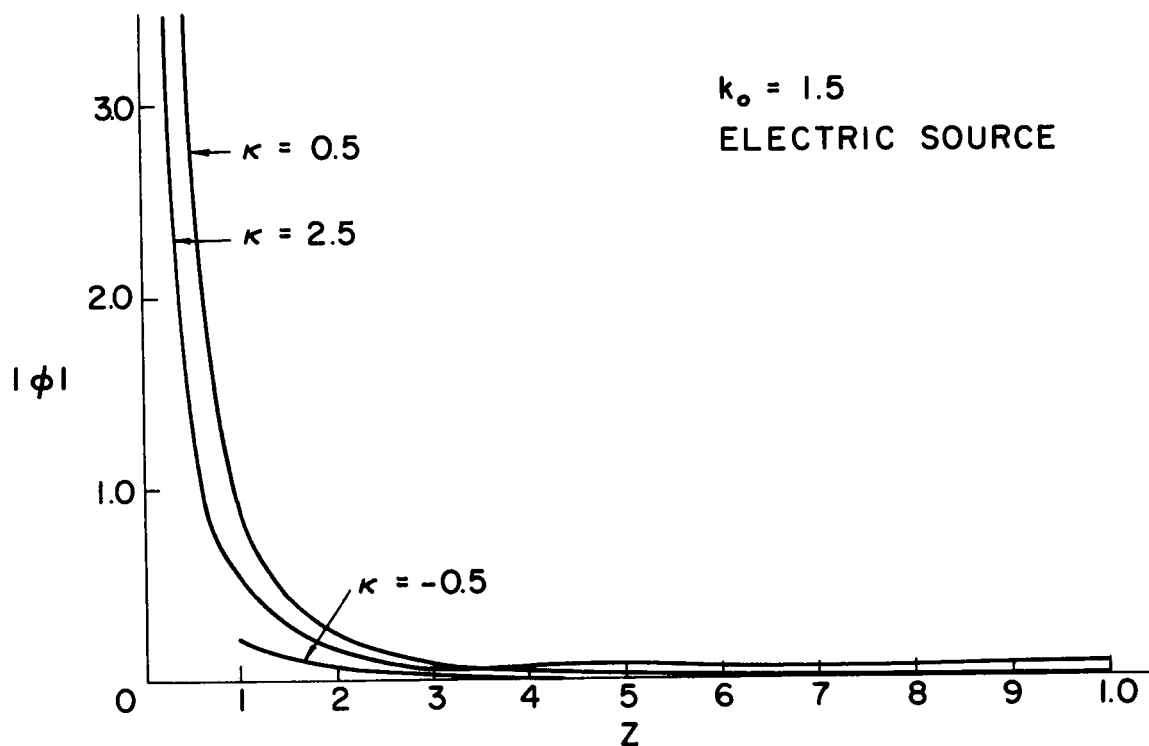


Figure 5(c). Magnitude of vector potential,  $k_0 = 1.5$ .

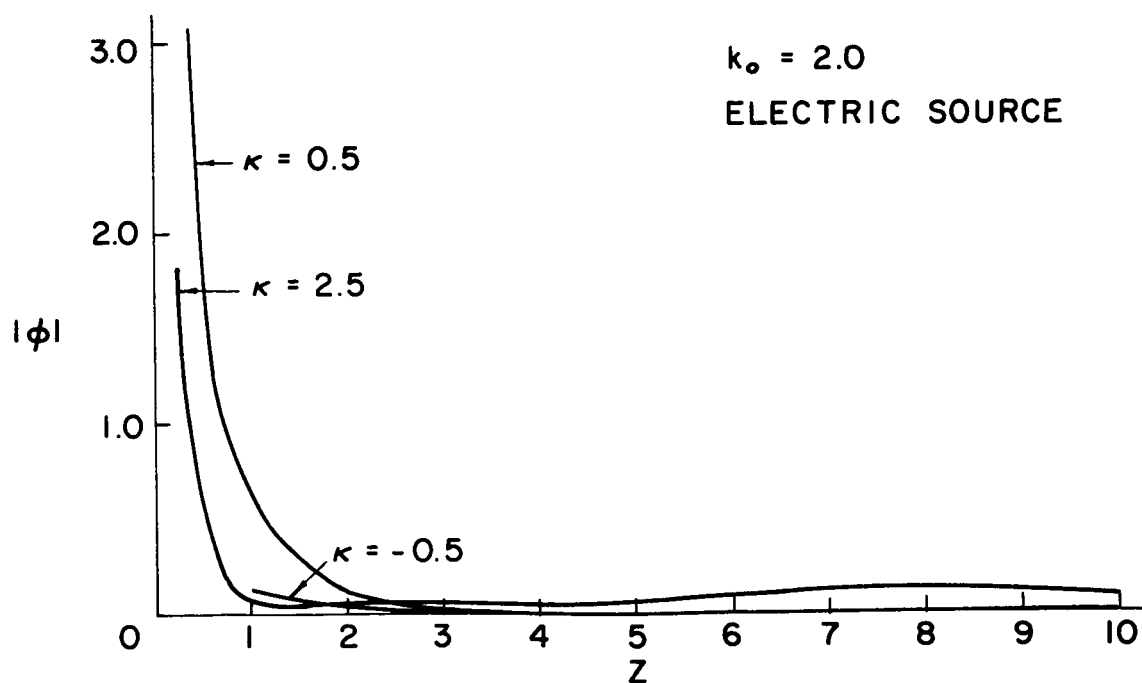


Figure 5(d). Magnitude of vector potential,  $k_0 = 2.0$ .

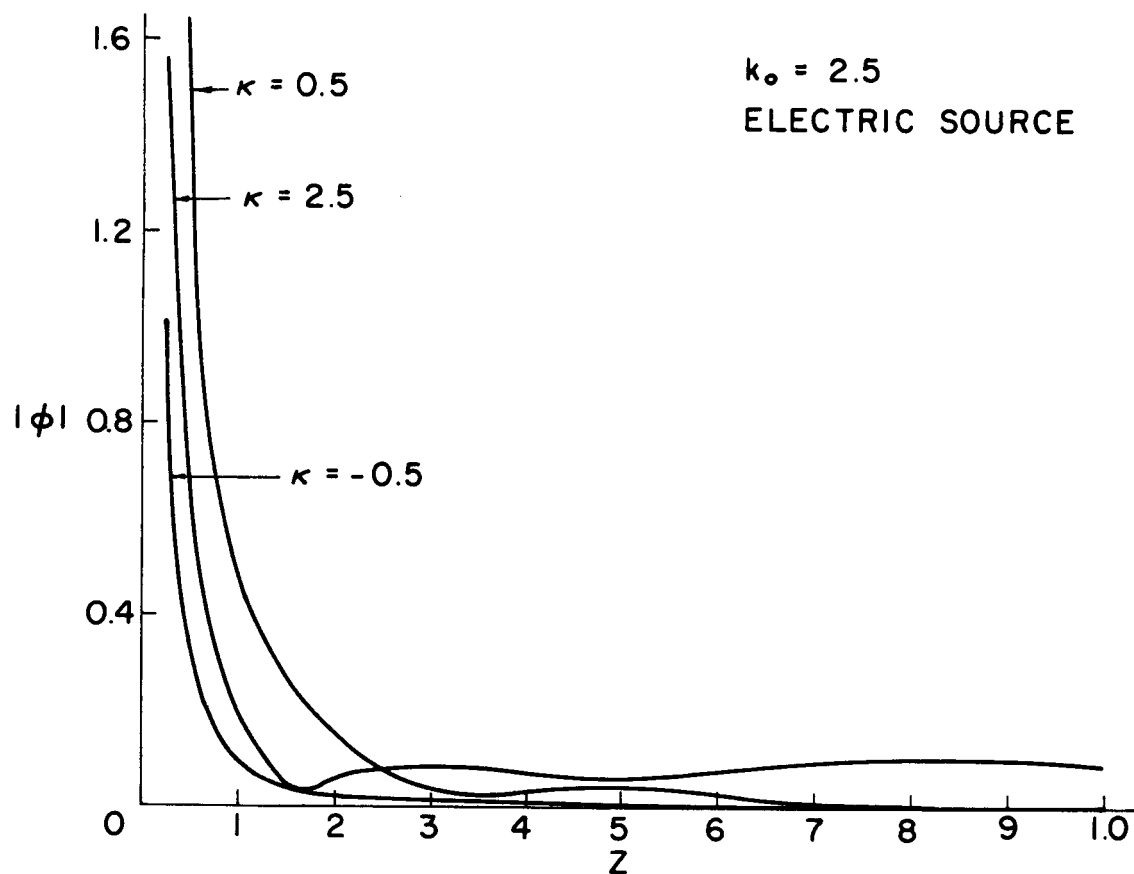


Figure 5(e). Magnitude of vector potential,  $k_0 = 2.5$ .

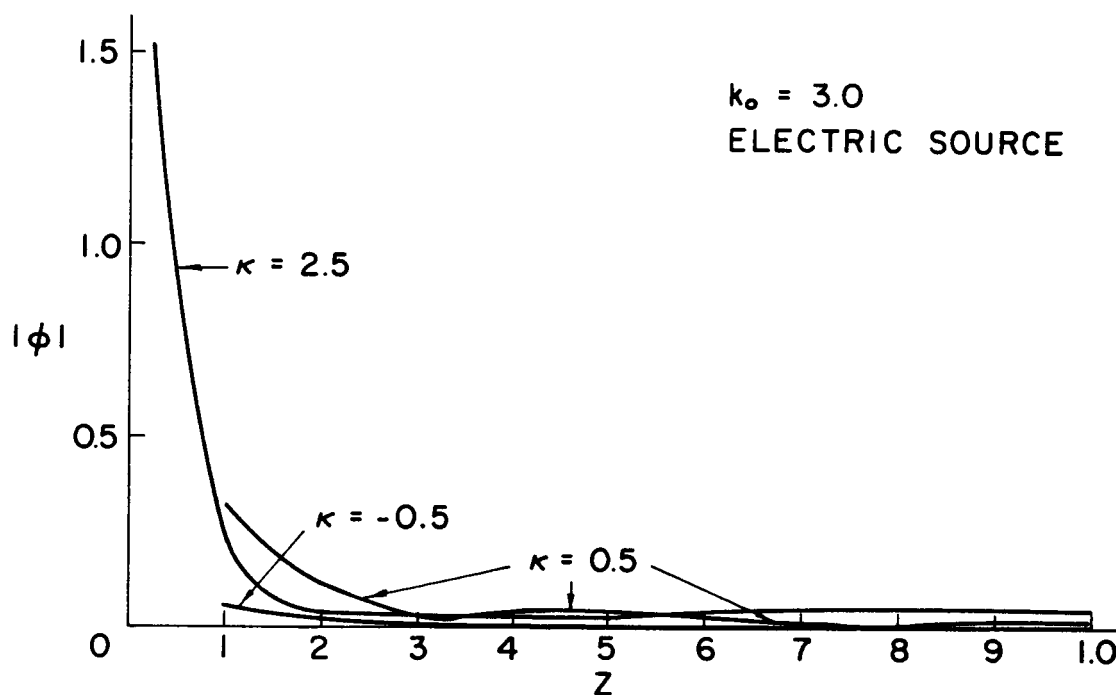


Figure 5(f). Magnitude of vector potential,  $k_0 = 3.0$ .



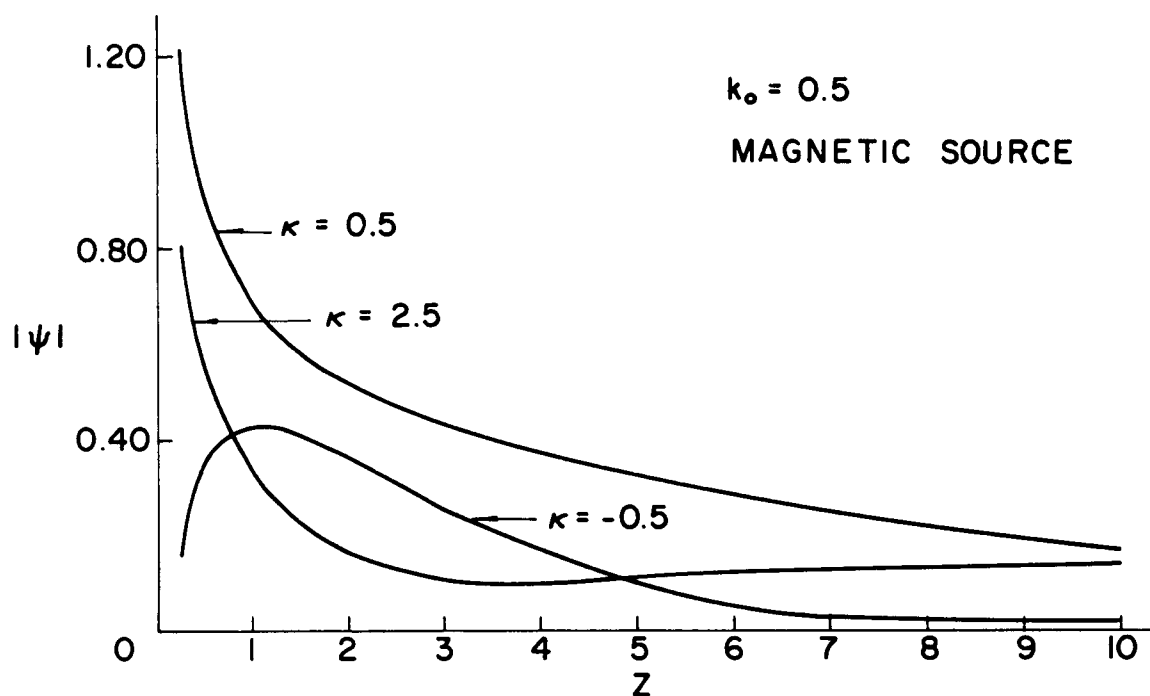


Figure 6(a). Magnitude of vector potential,  $k_o = 0.5$ .

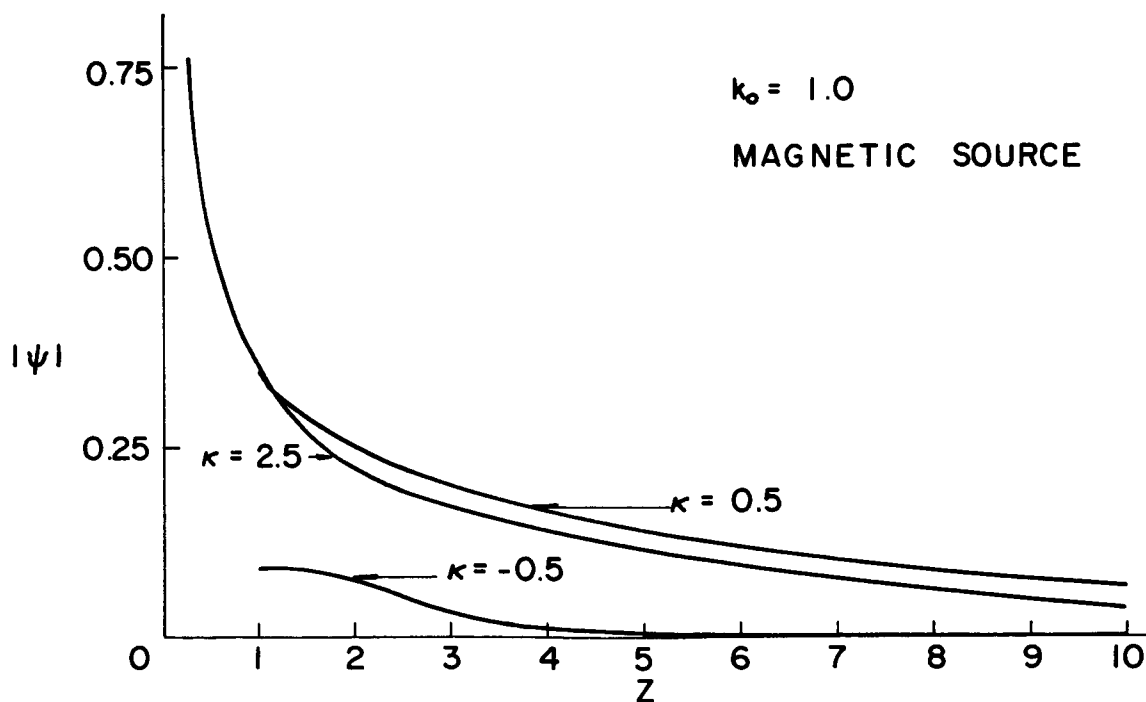


Figure 6(b). Magnitude of vector potential,  $k_o = 1.0$ .

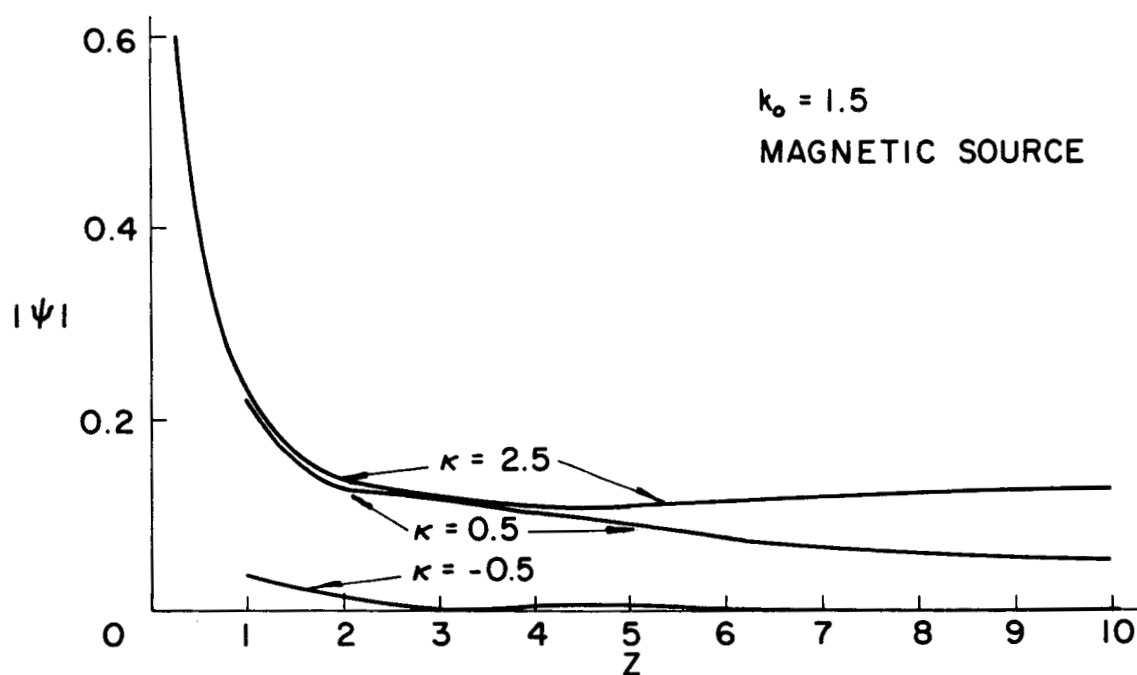


Figure 6(c). Magnitude of vector potential,  $k_0 = 1.5$ .

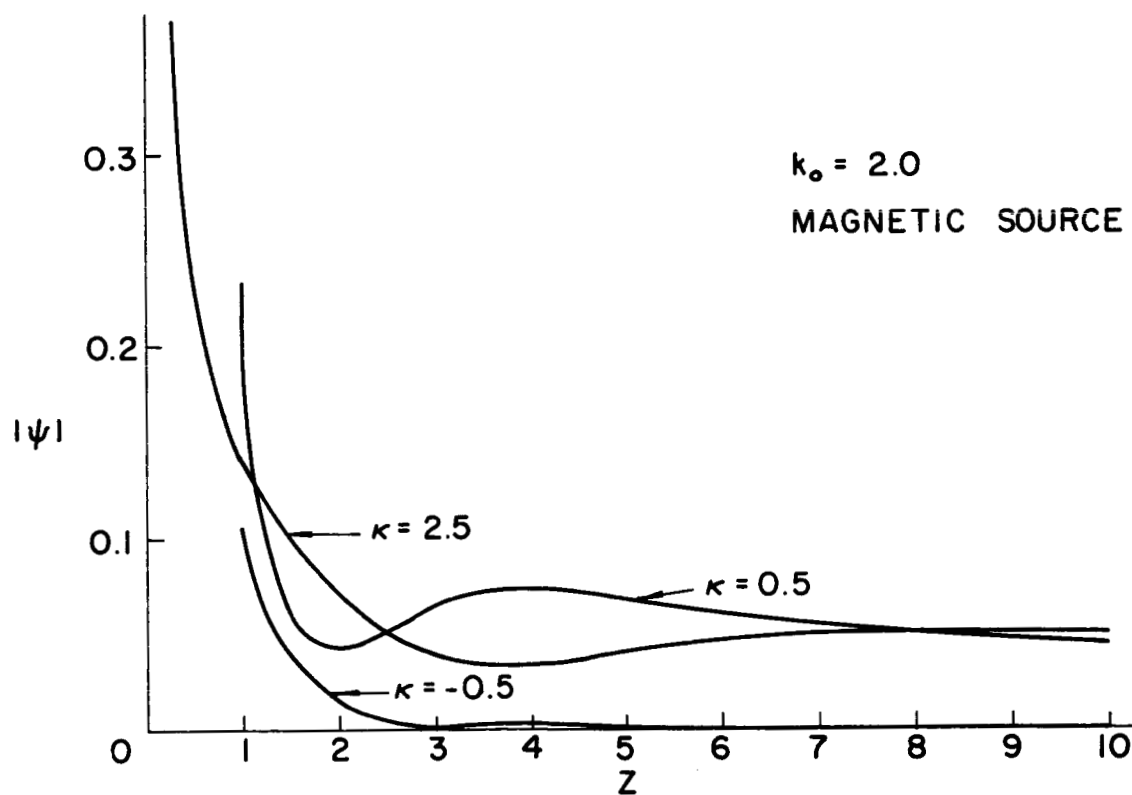


Figure 6(d). Magnitude of vector potential,  $k_0 = 2.0$ .

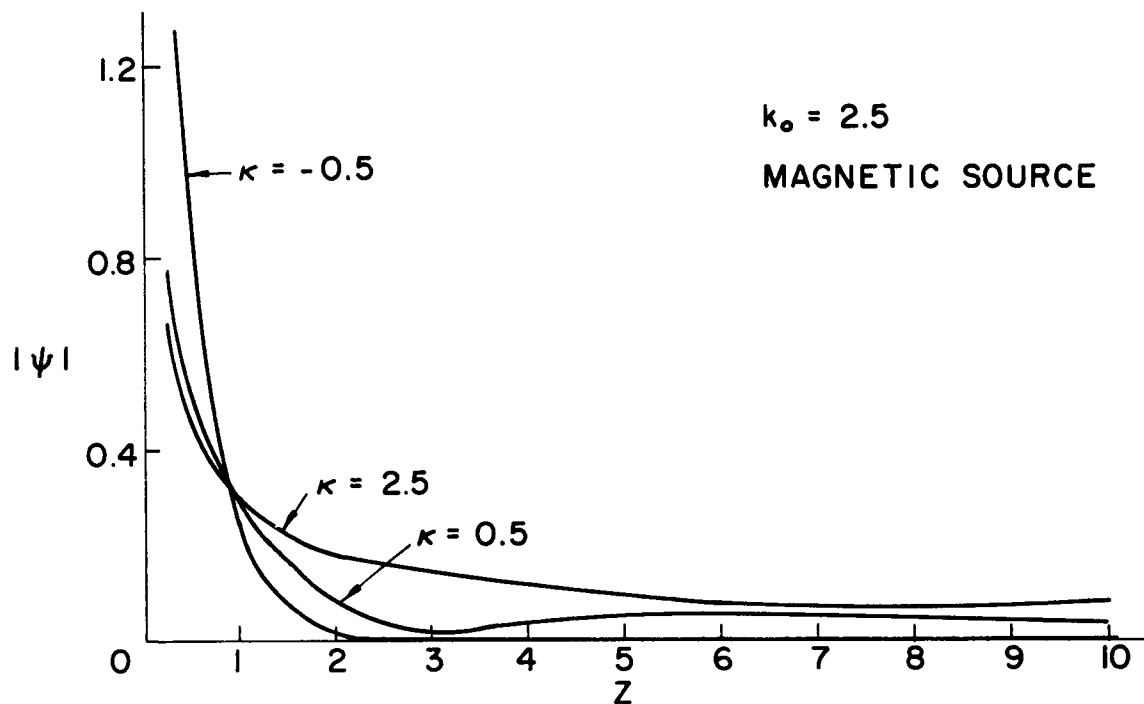


Figure 6(e). Magnitude of vector potential,  $k_0 = 2.5$ .

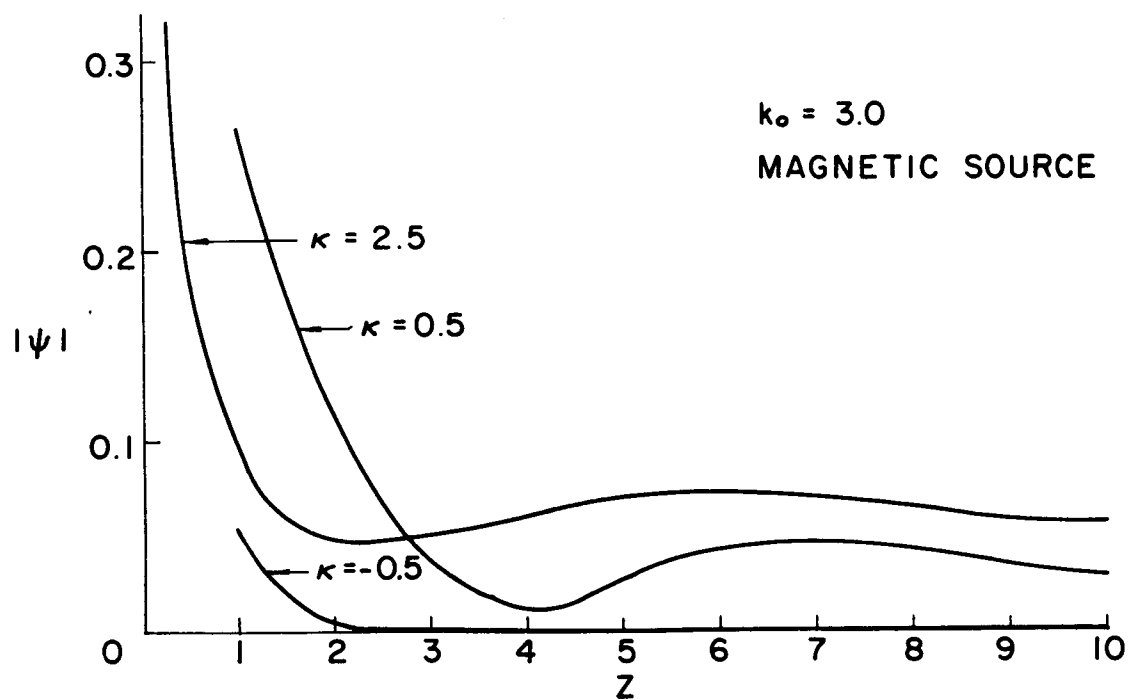


Figure 6(f). Magnitude of vector potential,  $k_0 = 3.0$ .

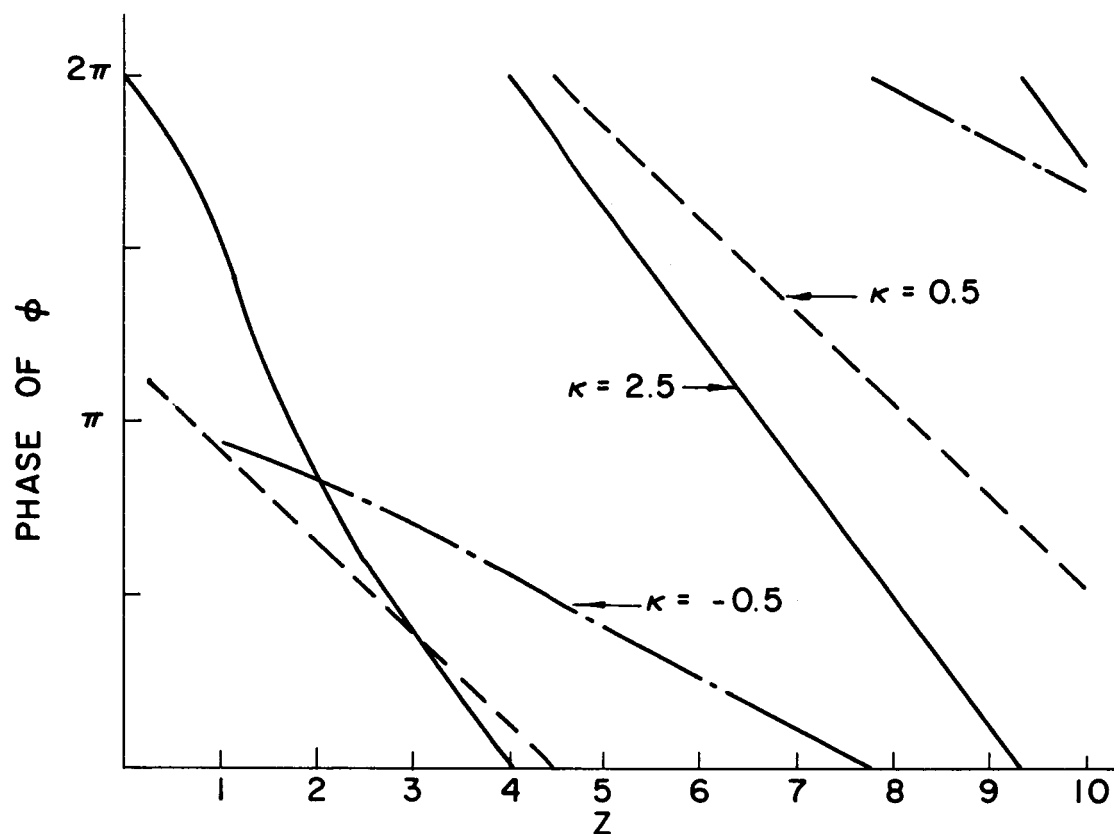


Figure 7(a). Phase of vector potential for electric source,  $k_0 = 1.0$ .

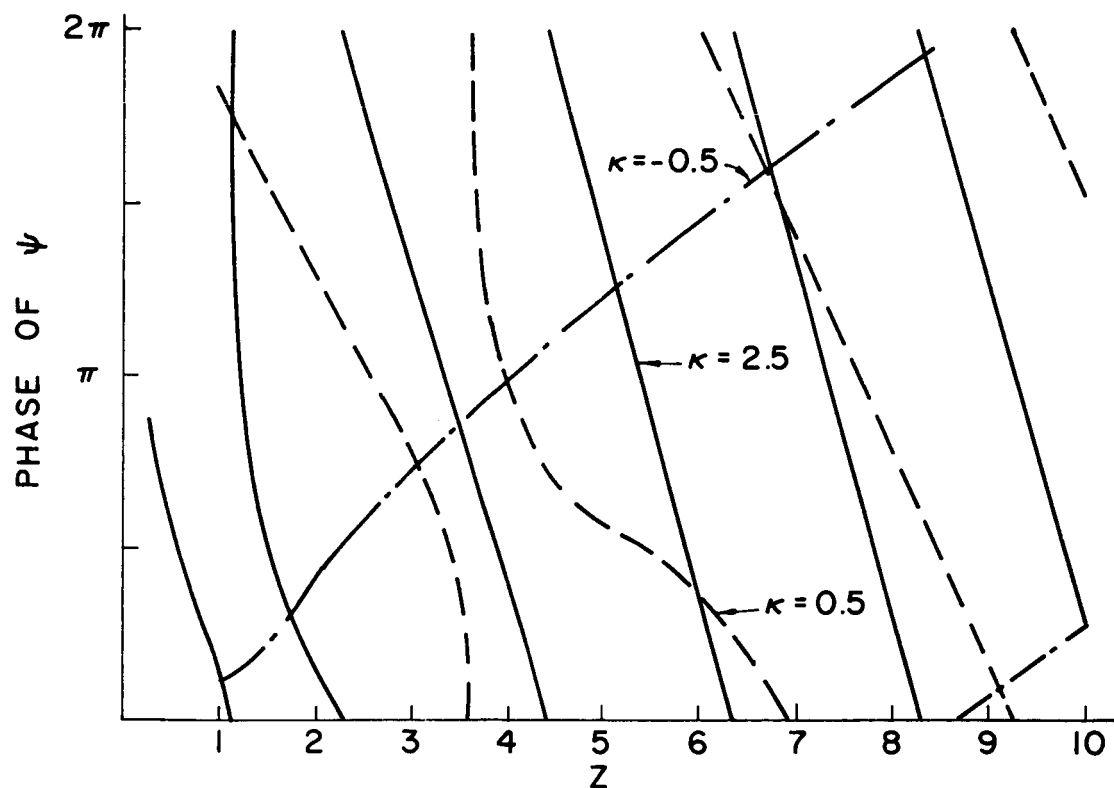


Figure 7(b). Phase of vector potential for magnetic source,  $k_0 = 3.0$ .

further suggests that such behavior may in fact hold for other cases, but this hypothesis has not been confirmed.

In Figures 8(a) and 8(b), the magnitude of the total vector potential is plotted along with the magnitude of the total traveling wave contribution to the field. That is, in the latter case, the integrals on  $C_A$  and  $C_B$ , which constitute the space wave, have been neglected. Because of the relative difficulty of computing such integrals numerically, it would be valuable to determine under what conditions the field can be suitably approximated by neglecting these integrals.

Computing the residue contribution for each set of parameters and comparing it with the total field indicates that, in most cases, the field along the surface may be reasonably approximated by the residue contribution alone for  $k_0 z > \pi$ , i.e., for  $z$  greater than one-half wavelength in free space. However, great caution must be exercised in those cases when only a few leaky wave poles are found. In addition, as was mentioned previously, other poles on the bottom sheet of the Riemann surface may contribute strongly to the field by influencing the behavior of the integrand along  $C_B$  if they lie near the path. In any event, careful investigation of poles in the bottom sheet on both sides of the path of integration is advisable before neglecting the contribution of the integrals along the two segments.

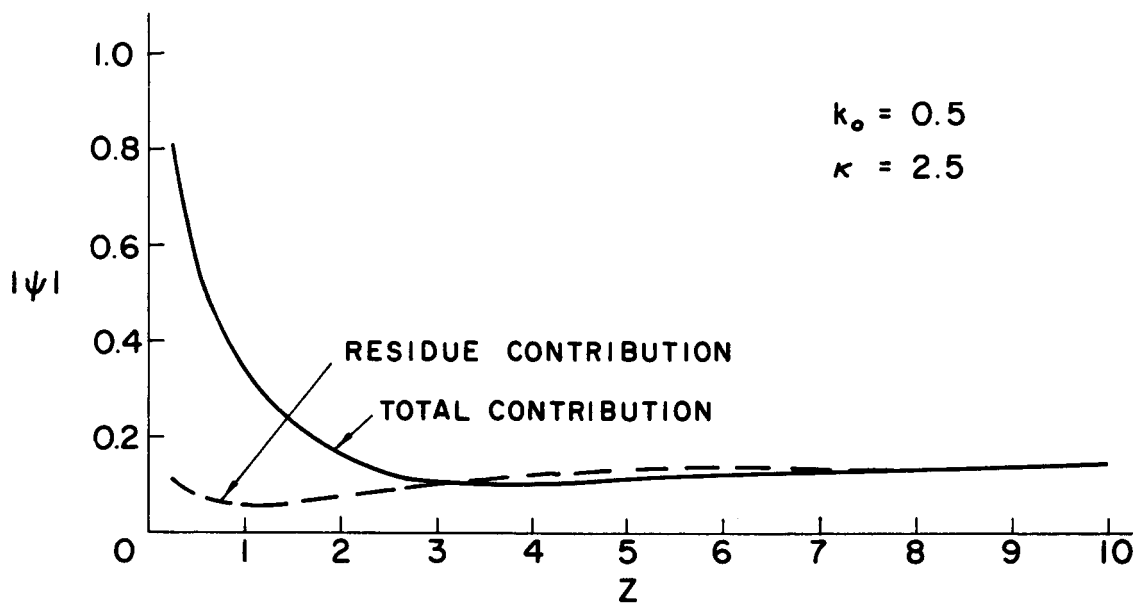


Figure 8(a). Residue contribution and total field,  $\kappa = 2.5$ .

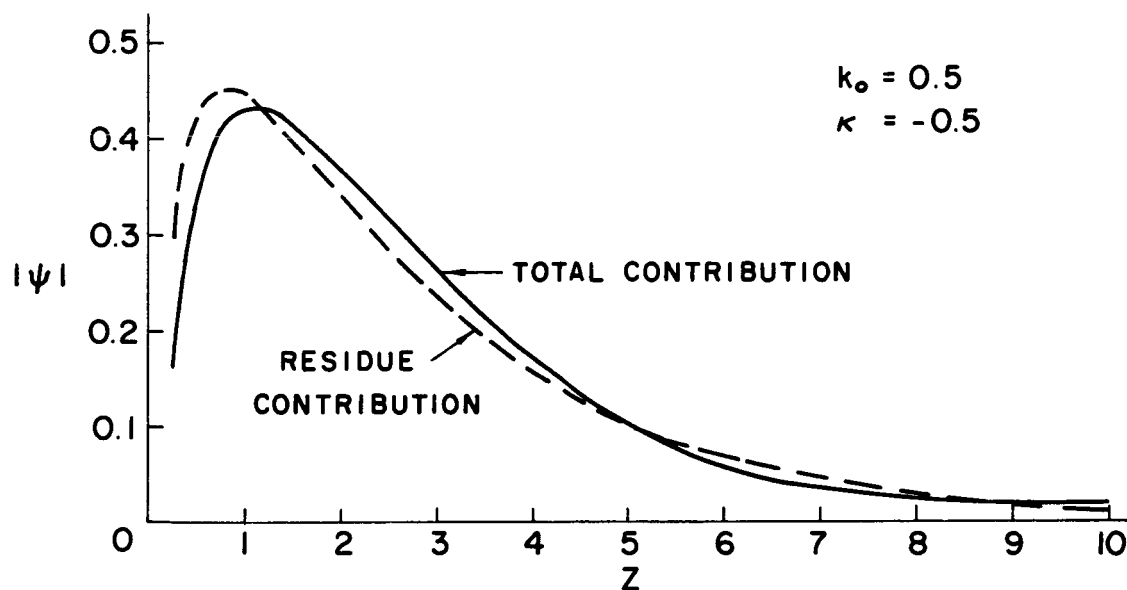


Figure 8(b). Residue contribution and total field,  $\kappa = -0.5$ .

## SUMMARY

The near fields for a grounded dielectric slab excited by a line source of magnetic or electric current were calculated for several frequencies and for dielectric constants of 2.5, 0.5 and - 0.5. The derivation of the solution in a Fourier inversion integral was obtained in a conventional approach, but the inversion of the transform was treated not by the usual saddle-point method, but by a very direct method in the plane of the complex transform variable  $\gamma$ .

The fields were determined in terms of a superposition of traveling waves plus a contribution given by the space wave. Fields were found in some cases as near as one-tenth wavelength to the source. In addition, conditions under which the field may reasonably be approximated by the traveling waves alone were discussed.

Possibilities for further study include treatment of the extreme near field by direct numerical integration of the complex inversion integral, but in particular, extension of the methods used in this problem to related problems in which an inversion integral must be evaluated approximately is suggested for further work.

## BIBLIOGRAPHY

1. Bates, Cyril P., "A Technique for Solving Certain Wiener-Hopf Type Boundary Value Problems," Ph.D. thesis, University of Illinois, Urbana, Illinois, 1966.
2. Collin, Robert E., Field Theory of Guided Waves, New York, 1960.
3. Hille, Einar, Analytic Function Theory, Vol. I, New York, 1959.
4. Norton, David E., "The Calculation and Measurements of the Near Fields of a Surface Waveguide," IEEE International Convention Record, Part 5, 1965, pp. 200-208.
5. McCracken, Daniel D. and Dorn, William S., Numerical Methods and FORTRAN Programming, New York, 1964.
6. Morse, Philip M. and Feshbach, Herman, Methods of Theoretical Physics, New York, 1953.



Unclassified  
Security Classification

DOCUMENT CONTROL DATA - R&D		
(Security classification of title, body of abstract and indexing annotation must be entered when the overall report is classified)		
1. ORIGINATING ACTIVITY (Corporate author)		2a. REPORT SECURITY CLASSIFICATION
University of Illinois, Urbana, Illinois		Unclassified
		2b. GROUP
3. REPORT TITLE		
A NEAR-FIELD SOLUTION FOR AN INFINITE LINE SOURCE ABOVE A DIELECTRIC COATED CONDUCTING PLANE		
4. DESCRIPTIVE NOTES (Type of report and inclusive dates)		
Interim Technical Report		
5. AUTHOR(S) (Last name, first name, initial)		
Van Blaricum, G. F. and Mittra, R.		
6. REPORT DATE	7a. TOTAL NO. OF PAGES	7b. NO. OF REFS
August 1966	35	6
8a. CONTRACT OR GRANT NO.	9a. ORIGINATOR'S REPORT NUMBER(S)	
AF19(628)-3819	Antenna Laboratory Report No.	
b. PROJECT AND TASK NO.	T. R. No. 10 66-13	
5635-02		
c. DOD ELEMENT	9b. OTHER REPORT NO(S) (Any other numbers that may be assigned this report)	
61445014	AFCRL-66-700	
d. DOD SUBELEMENT		
681305		
10. AVAILABILITY/LIMITATION NOTICES		
Distribution of this document is unlimited.		
11. SUPPLEMENTARY NOTES		12. SPONSORING MILITARY ACTIVITY
		Hq. AFCRL, OAR (CRD)
		United States Air Force
		L. G. Hanscom Field, Bedford, Mass.
13. ABSTRACT		
<p>The fields along a dielectric slab excited by a line source are found by considering the inversion integral of a Fourier transform directly rather than by resorting to the usual saddle point approximation techniques. The field at any point along the surface is expressed as a superposition of traveling waves plus a space-wave contribution, and conditions under which the field may be approximated by traveling wave components alone are discussed. Results of sample computations for both electric and magnetic current excitation are given.</p>		

DD FORM 1473  
1 JAN 64

Unclassified  
Security Classification

14.	KEY WORDS	LINK A		LINK B		LINK C	
		ROLE	WT	ROLE	WT	ROLE	WT
	Electromagnetic theory Antennas Surface waves Leaky waves Source excitation Dielectric coated conductor Plasma covered surface						

#### INSTRUCTIONS

1. ORIGINATING ACTIVITY: Enter the name and address of the contractor, subcontractor, grantee, Department of Defense activity or other organization (*corporate author*) issuing the report.

2a. REPORT SECURITY CLASSIFICATION: Enter the overall security classification of the report. Indicate whether "Restricted Data" is included. Marking is to be in accordance with appropriate security regulations.

2b. GROUP: Automatic downgrading is specified in DoD Directive 5200.10 and Armed Forces Industrial Manual. Enter the group number. Also, when applicable, show that optional markings have been used for Group 3 and Group 4 as authorized.

3. REPORT TITLE: Enter the complete report title in all capital letters. Titles in all cases should be unclassified. If a meaningful title cannot be selected without classification, show title classification in all capitals in parenthesis immediately following the title.

4. DESCRIPTIVE NOTES: If appropriate, enter the type of report, e.g., interim, progress, summary, annual, or final. Give the inclusive dates when a specific reporting period is covered.

5. AUTHOR(S): Enter the name(s) of author(s) as shown on or in the report. Enter last name, first name, middle initial. If military, show rank and branch of service. The name of the principal author is an absolute minimum requirement.

6. REPORT DATE: Enter the date of the report as day, month, year, or month, year. If more than one date appears on the report, use date of publication.

7a. TOTAL NUMBER OF PAGES: The total page count should follow normal pagination procedures, i.e., enter the number of pages containing information.

7b. NUMBER OF REFERENCES: Enter the total number of references cited in the report.

8a. CONTRACT OR GRANT NUMBER: If appropriate, enter the applicable number of the contract or grant under which the report was written.

8b, 8c, & 8d. PROJECT NUMBER: Enter the appropriate military department identification, such as project number, subproject number, system numbers, task number, etc.

9a. ORIGINATOR'S REPORT NUMBER(S): Enter the official report number by which the document will be identified and controlled by the originating activity. This number must be unique to this report.

9b. OTHER REPORT NUMBER(S): If the report has been assigned any other report numbers (*either by the originator or by the sponsor*), also enter this number(s).

10. AVAILABILITY/LIMITATION NOTICES: Enter any limitations on further dissemination of the report, other than those imposed by security classification, using standard statements such as:

- (1) "Qualified requesters may obtain copies of this report from DDC."
- (2) "Foreign announcement and dissemination of this report by DDC is not authorized."
- (3) "U. S. Government agencies may obtain copies of this report directly from DDC. Other qualified DDC users shall request through \_\_\_\_\_."
- (4) "U. S. military agencies may obtain copies of this report directly from DDC. Other qualified users shall request through \_\_\_\_\_."
- (5) "All distribution of this report is controlled. Qualified DDC users shall request through \_\_\_\_\_."

If the report has been furnished to the Office of Technical Services, Department of Commerce, for sale to the public, indicate this fact and enter the price, if known.

11. SUPPLEMENTARY NOTES: Use for additional explanatory notes.

12. SPONSORING MILITARY ACTIVITY: Enter the name of the departmental project office or laboratory sponsoring (*paying for*) the research and development. Include address.

13. ABSTRACT: Enter an abstract giving a brief and factual summary of the document indicative of the report, even though it may also appear elsewhere in the body of the technical report. If additional space is required, a continuation sheet shall be attached.

It is highly desirable that the abstract of classified reports be unclassified. Each paragraph of the abstract shall end with an indication of the military security classification of the information in the paragraph, represented as (TS), (S), (C), or (U).

There is no limitation on the length of the abstract. However, the suggested length is from 150 to 225 words.

14. KEY WORDS: Key words are technically meaningful terms or short phrases that characterize a report and may be used as index entries for cataloging the report. Key words must be selected so that no security classification is required. Identifiers, such as equipment model designation, trade name, military project code name, geographic location, may be used as key words but will be followed by an indication of technical context. The assignment of links, rules, and weights is optional.